

Published in final edited form as:

Nature. 2013 May 16; 497(7449): 383–387. doi:10.1038/nature12080.

EGFR modulates microRNA maturation in response to hypoxia through phosphorylation of AGO2

Jia Shen^{1,2}, Weiya Xia¹, Yekaterina B. Khotskaya¹, Longfei Huo¹, Kotaro Nakanishi³, Seung-Oe Lim¹, Yi Du^{1,2}, Yan Wang¹, Wei-Chao Chang^{4,5}, Chung-Hsuan Chen⁵, Jennifer L. Hsu^{1,4,6}, Yun Wu⁷, Yung Carmen Lam¹, Brian P. James⁸, Xiuping Liu⁸, Chang-Gong Liu⁸, Dinshaw J. Patel³, and Mien-Chie Hung^{1,2,4,6}

¹Department of Molecular and Cellular Oncology, The University of Texas MD Anderson Cancer Center, 1515 Holcombe Boulevard, Houston, Texas 77030, USA

²The University of Texas Graduate School of Biomedical Sciences at Houston, Houston, Texas 77030, USA

³Structural Biology Program, Memorial Sloan-Kettering Cancer Center, New York, New York 10065, USA

⁴Center for Molecular Medicine and Graduate Institute of Cancer Biology, China Medical University, Taichung 402, Taiwan

⁵Genomics Research Center, Academia Sinica, Nankang, Taipei 105, Taiwan

⁶Asia University, Taichung 413, Taiwan

⁷Department of Pathology, The University of Texas MD Anderson Cancer Center, 1515 Holcombe Boulevard, Houston, Texas 77030, USA

⁸Department of Experimental Therapeutics, The University of Texas MD Anderson Cancer Center, 1515 Holcombe Boulevard, Houston, Texas 77030, USA

Abstract

MicroRNAs (miRNAs) are generated by two-step processing to yield small RNAs that negatively regulate target gene expression at the post-transcriptional level¹. Deregulation of miRNAs has been linked to diverse pathological processes, including cancer^{2,3}. Recent studies have also implicated miRNAs in the regulation of cellular response to a spectrum of stresses⁴, such as hypoxia, which is frequently encountered in the poorly angiogenic core of a solid tumour⁵. However, the upstream regulators of miRNA biogenesis machineries remain obscure, raising the question of how tumour cells efficiently coordinate and impose specificity on miRNA expression and function in response to stresses. Here we show that epidermal growth factor receptor (EGFR), which is the product of a well-characterized oncogene in human cancers, suppresses the

©2013 Macmillan Publishers Limited. All rights reserved

Correspondence and requests for materials should be addressed to M.-C.H. (mhung@mdanderson.org).

Supplementary Information is available in the online version of the paper.

Author Contributions J.S. and M.-C.H. designed and conceived the study; J.S. and M.-C.H. wrote the manuscript; J.L.H. contributed to the preparation of the manuscript. J.S., W.X., Y.B.K., L.H., S.-O.L., Y.D., Y. Wang, W.-C.C. and C.-H.C. did the experiments; Y. Wu provided human primary breast tumour samples; Y.C.L. provided the split-half-YFP-fused constructs; X.L. and C.-G.L. assisted in next-generation RNA deep sequencing; B.P.J. provided the pipeline analysis service for RNA sequencing data; and K.N. and D.-J.P. analysed the crystal structure of human AGO2.

Reprints and permissions information is available at www.nature.com/reprints.

The authors declare no competing financial interests.

Readers are welcome to comment on the online version of the paper.

maturation of specific tumour-suppressor-like miRNAs in response to hypoxic stress through phosphorylation of argonaute 2 (AGO2) at Tyr 393. The association between EGFR and AGO2 is enhanced by hypoxia, leading to elevated AGO2-Y393 phosphorylation, which in turn reduces the binding of Dicer to AGO2 and inhibits miRNA processing from precursor miRNAs to mature miRNAs. We also identify a long-loop structure in precursor miRNAs as a critical regulatory element in phospho-Y393-AGO2-mediated miRNA maturation. Furthermore, AGO2-Y393 phosphorylation mediates EGFR-enhanced cell survival and invasiveness under hypoxia, and correlates with poorer overall survival in breast cancer patients. Our study reveals a previously unrecognized function of EGFR in miRNA maturation and demonstrates how EGFR is likely to function as a regulator of AGO2 through novel post-translational modification. These findings suggest that modulation of miRNA biogenesis is important for stress response in tumour cells and has potential clinical implications.

Activated EGFR contained in intracellular vesicles is capable of activating intracellular signalling pathways before lysosomal degradation⁶. Importantly, proteins associating with internalized EGFR probably differ from those transducing signalling at the plasma membrane⁷, suggesting a higher degree of signalling complexity that is not well characterized. We identified AGO2 as a novel EGFR-interacting protein by mass spectrometric analysis (Supplementary Fig. 1), and validated their association by co-immunoprecipitation and pull-down assays (Supplementary Fig. 2). The juxtamembrane and kinase domain of EGFR is essential for binding with AGO2 at the aminoterminal region.

Human AGO2 was initially reported as a membrane-associated cytoplasmic protein⁸ and is the catalytic centre of RNA-induced silencing complex⁹ (RISC). AGO2 also associates with Dicer and TRBP (HIV-1 transactivating response RNA-binding protein, also known as TARBP2) to form the RISC-loading complex, which is involved in the second step of miRNA processing from precursor to mature miRNAs^{10,11}. To investigate the physiological role of EGFR–AGO2 interaction, we screened different upstream EGFR-activating stimuli, including ligands and stresses^{12–15}, in HTC-1080 stable clone expressing split-half-YFP-fused EGFR and AGO2 (EGFR with the N-terminal domain of YFP fused to the C terminus and AGO2 with C-terminal domain of YFP fused to the C terminus; Supplementary Fig. 3a; YFP, yellow fluorescent protein), in which the YFP fluorescence can be reconstituted only on protein–protein association¹⁶ (Fig. 1a). Of the four different types of stimuli, hypoxic stress induced the strongest level of YFP fluorescence (Supplementary Figs 3b, c and 4), with distinct foci formed in cytoplasm (Fig. 1b), suggesting that internalized EGFR interacts with AGO2 in aggregates. Dynamic EGFR–AGO2 association was further validated in HeLa cells and various cancer cell lines by co-immunoprecipitation (Fig. 1c and Supplementary Fig. 5) and co-localization assays (Supplementary Figs 6 and 7), and was found to be RNase resistant (Supplementary Fig. 8), indicating that EGFR and AGO2 are direct physical interacting partners *in vivo*.

Hypoxia is known to upregulate EGFR¹⁴ and prolong its activation through retention in endocytic trafficking¹³. Indeed, hypoxia enhanced EGFR expression in late endosomes (multivesicular bodies; Supplementary Fig. 9, F2–F4), where it co-localized with AGO2 (Supplementary Fig. 10 and Fig. 1d) and co-fractionated (Supplementary Fig. 9) with RISC components (AGO2, DCP1A and GW182) as well as the RISC-loading complex (Dicer, TRBP and AGO2). Silencing GRB2, a key modulator of EGFR endocytosis¹⁷, diminished EGFR–AGO2 interaction (Supplementary Fig. 11), highlighting the importance of internalization. Furthermore, inhibition or silencing of hypoxia-inducible transcriptional factors¹⁸ (HIF1 α (HIF1A) and HIF2 α (EPAS1)) reduced EGFR–AGO2 association (Supplementary Fig. 12a and Fig. 1e) and co-localization (Supplementary Figs 12b and 13) under hypoxia, and stabilization of HIF1 α and HIF2 α (HIF1/2 α) triggered the interaction of

EGFR and AGO2 under normoxia (Supplementary Fig. 14). Nonetheless, EGFR–AGO2 association in RCC4 cells (endogenous VHL null with constitutively expressed HIF1/2 α) was further strengthened by hypoxia regardless of the exogenous expression of wild-type VHL (Supplementary Fig. 15). These results indicate that stable expression of HIF1/2 α is sufficient to trigger EGFR–AGO2 interaction that is further enhanced by hypoxia, probably through an HIF1/2 α -independent mechanism.

To assess the functional importance of EGFR–AGO2 interaction in miRNA regulation, we profiled RNA expression in HeLa stable clones expressing scrambled control or short hairpin RNA (shRNA) against EGFR under normoxia or hypoxia by RNA deep sequencing (Supplementary Figs 16a and 17). Hierarchical clustering analysis of relative expression of precursor and mature miRNAs (scrambled versus shRNA against EGFR; Supplementary Fig. 16b) identified one distinct cluster of miRNAs under hypoxia (Fig. 2a, dashed box). In the presence of EGFR, the level of precursor miRNAs increased with a concomitant decrease in the expression of mature miRNAs. However, the maturation of this cluster of miRNAs was not significantly altered by EGFR under normoxia (Fig. 2a), implying that their processing from precursor to mature miRNAs was negatively regulated by EGFR specifically in response to hypoxia. We defined this subcluster of miRNAs as mHESM (miRNAs regulated by hypoxia-dependent EGFR-suppressed maturation). We then pooled mHESM and narrowed down the candidates on the basis of their absolute mature miRNA expression affected by EGFR knockdown. A majority of the top-scoring mHESM turned out to have tumour suppressor characteristics^{3,4,19–21} (Fig. 2a).

To determine the functional relevance of mHESM, messenger RNAs (mRNAs) regulated by EGFR were sorted and overlapped with the predicted mRNA targets of top-scoring mHESM, revealing 439 mRNAs (Supplementary Data) that are regulated by EGFR and also targeted by top-scoring mHESM (Fig. 2b). In response to hypoxia, EGFR reduced the production of mHESM but enhanced the expression of corresponding mRNA targets (Fig. 2b), which is evidence of the importance of EGFR-modulated miRNA maturation. The inhibitory role of EGFR in miRNA maturation in response to hypoxia was further validated in HeLa stable transfectants expressing scrambled control or shRNAs targeting EGFR (Supplementary Fig. 19) by quantitative PCR. Moreover, induction of wild-type but not kinase-dead EGFR in HeLa Tet-Off-inducible stable clones (Supplementary Fig. 20a) inhibited the maturation of top-scoring mHESM in response to hypoxia (Supplementary Figs 20b,c), suggesting that EGFR kinase activity is important for EGFR-suppressed miRNA maturation.

To investigate whether AGO2 is a phosphorylation substrate of EGFR, we purified FLAG-tagged AGO2 co-expressed with EGFR and identified one Tyr phosphorylation site (Supplementary Fig. 21) at a highly conserved residue, Tyr 393 (Supplementary Fig. 22), in AGO2. Results from *in vitro* kinase assay (Fig. 3a) further demonstrated AGO2-Y393 to be a direct phosphorylation site targeted by EGFR. Mutational analysis suggested that phospho-Y393-AGO2 exists *in vivo* (Supplementary Figs 23 and 24), and this was validated in HeLa Tet-Off-inducible AGO2 stable clones (Supplementary Fig. 25a and Fig. 3b) using the polyclonal antibody (p-Y393-AGO2) we generated (Supplementary Fig. 26). Notably, hypoxia enhanced AGO2-Y393 phosphorylation (Fig. 3b), which in turn reduced the association of AGO2 with Dicer and TRBP (Fig. 3b and Supplementary Figs 23 and 24), suggesting that EGFR is a novel upstream regulator of the RISC-loading complex.

To gain more insight into phospho-Y393-AGO2, we analysed the crystal structure of AGO2 (refs 22 and 23) and found that the side chain of Tyr 393 protrudes with an exterior orientation towards a cavity between the N domain (an interaction surface for EGFR) and the linker L2 (a linker domain between PAZ and MID) (Fig. 3c). Tyr 393 is exposed to

solvent and is some distance from both the guide RNA-binding channel and the PIWI box, a Dicer-binding region of AGO2 (ref. 24). Given that Dicer is a large protein, it is conceivable that Dicer could still interact with both the Dicer-specific PIWI box and Tyr 393 owing to their location on the same surface of AGO2 (Fig. 3c). If so, phosphorylation of Tyr 393 could inhibit this interaction as previously observed (Fig. 3b and Supplementary Figs 23 and 24).

The recruitment of AGO2 to Dicer is critical for loading miRNA precursors onto the RISC-loading complex²⁵ and facilitating miRNA maturation^{11,25} from precursor to mature miRNAs. We therefore investigated whether AGO2-Y393 phosphorylation has a role in EGFR-suppressed miRNA maturation in response to hypoxia. Compared with an AGO2-Y393F mutant, induction of wild-type AGO2 (AGO2-WT) significantly reduced the expression of most mHESM but not those that do not belong to the mHESM cluster (defined as non-mHESM) in response to hypoxia (Supplementary Fig. 25b). Structural analysis of miRNA precursors determined that a majority of mHESM regulated by p-Y393-AGO2 contained a long-loop structure, which is not present in non-mHESM (Supplementary Fig. 25b). Notably, mHESM that were not significantly affected by AGO2-Y393 phosphorylation also had short-loop structures in their precursors, similar to what we found in non-mHESM (Supplementary Fig. 25b). This suggests that long-loop structure is important in regulation specificity. Similar expression patterns of mature miRNAs were observed in other paired stable clones (Supplementary Figs 27 and 28).

Silencing endogenous EGFR significantly diminished the expression difference of long-loop mHESM present in miR-31, miR-192 and miR-193a-5p between AGO2-WT and AGO2-Y393F mutant cells (Supplementary Fig. 29). The levels of their primary transcripts were reduced by EGFR knockdown under hypoxia but were similar in AGO2-WT and AGO2-Y393F cells (Supplementary Fig. 29b). This is evidence that EGFR is a tyrosine kinase that mediates phospho-Y393-AGO2-suppressed miRNA maturation under hypoxia. Moreover, decreased expression of long-loop mHESM as shown in miR-31, miR-192 and miR-193a-5p under hypoxia resulted in the de-repression of miRNA targets (Fig. 3d) as measured by miR-reporter luciferase activity. In contrast, the expression of miR-21 (non-mHESM) and the repression of its target were not significantly affected by AGO2-Y393 phosphorylation (Fig. 3d). These results underline the functional importance of p-Y393-AGO2-mediated suppression of long-loop mHESM under hypoxia.

The long-loop structure in miRNA precursors is a known characteristic of Dicer's preference in substrate recognition²⁶. Reduction in the Dicer-AGO2 interaction resulted in less loading of the precursors of miR-31, miR-192 and miR-193a-5p (long-loop mHESM), but not that of miR-21 (short-loop non-mHESM), onto p-Y393-AGO2 under hypoxia (Supplementary Fig. 30). To examine the functional relevance of decreased Dicer-phospho-AGO2 association, we knocked down Dicer in HeLa Tet-Off-inducible AGO2 stable clones (Supplementary Fig. 31a, b and Fig. 3e) and found that the differences between AGO2-WT and AGO2-Y393F in miRNA precursor loading (Fig. 3e) and mature miRNA expression (Supplementary Fig. 31c) were significantly diminished. These results suggest that the maturation of long-loop mHESM is suppressed by AGO2-Y393 phosphorylation through Dicer. Moreover, AGO2-Y393F was capable of loading more mature mHESM (Fig. 3e), which is consistent with its enhanced RISC activity as indicated by luciferase reporter assay (Fig. 3d). However, the mature miRNA loading difference between AGO2-WT and AGO2-Y393F was Dicer dependent (Fig. 3e), and similar to what we observed in mature miRNA expression (Supplementary Fig. 31c). These data suggest that AGO2-Y393 phosphorylation decreases Dicer-AGO2 interaction, which in turn reduces miRNA precursor loading, suppresses the maturation of long-loop mHESM and decreases the loading of corresponding mature miRNAs onto RISC under hypoxia.

To demonstrate that the long-loop structure of precursor miRNAs indeed serves as one of the determinants that distinguish mHESM that are regulated by p-Y393-AGO2 from other miRNAs that are not, we mutated pre-miR-192-WT (long loop) into pre-miR-192-3M (short loop) and stably expressed them in HeLa Tet-Off-inducible AGO2 stable clones (Fig. 3f, top). Compared with AGO2-Y393F mutant, induction of AGO2-WT attenuated the maturation of pre-miR-192-WT but not pre-miR-192-3M, which virtually lost its processing efficacy without the long-loop structure (Fig. 3f and Supplementary Fig. 32). Conversely, AGO2-WT was able to suppress pre-miR-21-3M with a regenerated long-loop structure (Fig. 3g and Supplementary Fig. 33) that is not present in miR-21-WT (Fig. 3g and Supplementary Fig. 34). These results support a long-loop-dependent mechanism by which p-Y393-AGO2 confers regulation specificity on miRNA maturation.

The hypoxic tumour microenvironment promotes the metastatic phenotype by facilitating tumour cell survival through evasion of apoptosis¹⁸. Given that most mHESM suppressed by p-Y393-AGO2 are tumour-suppressor-like (Supplementary Figs 18 and 25b), we further investigated the pathophysiological role of AGO2 phosphorylation in response to hypoxia. Compared with vector control and AGO2-WT, a higher proportion of cells expressing AGO2-Y393F mutant underwent apoptosis following hypoxia exposure for three days (Supplementary Fig. 35), indicating that they were more susceptible to hypoxic stress. Knockdown of endogenous EGFR reduced cell survival and diminished the differences in apoptosis between AGO2-WT and AGO2-Y393F stable transfectants (Fig. 4a), suggesting that the phosphorylation of AGO2, rather than the mutation itself, is critical for cell survival under hypoxia. We did not observe any significant changes between AGO2-WT and AGO2-Y393F mutant in cell proliferation rate (Supplementary Fig. 36a, b) or anchorage-independent growth (Supplementary Fig. 36c, d). Notably, AGO2-WT but not AGO2-Y393F mutant significantly increased cell migration in response to hypoxia (Fig. 4b and Supplementary Figs 37 and 38). Treatment with Tyr-kinase inhibitor abrogated AGO2-WT-enhanced migration but failed to inhibit AGO2-Y393F mutant cells, indicating that AGO2-Y393 phosphorylation is important for EGFR-enhanced cell migration under hypoxia. Similar results were obtained from three-dimensional invasion assay with or without Tyr-kinase inhibitor treatment (Fig. 4c and Supplementary Fig. 39). These results demonstrate the functional importance of AGO2-Y393 phosphorylation in blocking cell apoptosis and enhancing cell invasiveness under hypoxia.

Finally, we used an orthotopic xenograft breast cancer model to establish the relationship between hypoxia, EGFR and p-Y393-AGO2, and showed that p-Y393-AGO2 along with EGFR is upregulated during tumour progression and specifically enriched in hypoxic tumour areas (Supplementary Fig. 40). To further examine the clinical relevance of AGO2-Y393 phosphorylation, we analysed the expression patterns of p-Y393-AGO2 and EGFR and the degree of hypoxia (indicated by HIF1 α and HIF2 α ; ref. 18) in primary breast tumours in consecutive sections collected from 128 human breast cancer patients. In adjacent normal breast tissues the expression of p-Y393-AGO2 was low, but in hypoxic breast tumours it was highly elevated (Fig. 4d). We observed significant positive correlations between p-Y393-AGO2, EGFR, HIF1 α and HIF2 α (Supplementary Fig. 41a and Supplementary Table 1) and further validated that AGO2-Y393 phosphorylation was enriched in hypoxic subareas of breast tumours with positive expression of EGFR (Supplementary Fig. 41b). Moreover, higher expression of p-Y393-AGO2 correlated significantly with poorer overall survival in breast cancer patients (Fig. 4e), supporting its clinical importance as a potential prognostic marker for breast cancer patient survival.

In this study, we identified a novel role for EGFR in miRNA maturation via AGO2-Y393 phosphorylation. Although these results suggest that EGFR is the Tyr kinase that suppresses miRNA maturation through AGO2-Y393 phosphorylation under hypoxia, there may be

other Tyr kinases that can also contribute to phospho-AGO2-mediated miRNA processing. The work we present here opens a new direction to understanding further the regulation of miRNA machinery in response to stress signalling, which is likely to have important clinical implications.

METHODS SUMMARY

We used quantitative PCR with reverse transcription to measure the expression levels of precursor and mature miRNAs, as described previously²⁷. Customized next-generation RNA deep sequencing, including both small-RNA application and whole-transcriptome analysis, was performed according to the standard protocol (Applied Biosystems). The full methodology can be found in Supplementary Information.

Supplementary Material

Refer to Web version on PubMed Central for supplementary material.

Acknowledgments

We thank B. Pickering, D. Yu, and A.-B. Shyu for suggestions and technical assistance with northern blot analysis. This work was supported by the US National Institutes of Health (CA109311 and CA099031 to M.-C.H., and CCSG Core Grant CA16672), the US National Breast Cancer Foundation, The Center for Biological Pathway at the UT MD Anderson Cancer Center, S. G. Komen (SAC110016 to M.-C.H.), The Sister Institution Fund of China Medical University and Hospital and the UT MD Anderson Cancer Center, the Cancer Research Center of Excellence (DOH102-TD-C-111-005, Taiwan), a Private University grant (NSC99-2632-B-039-001-MY3, Taiwan), and the Program for Stem Cell and Regenerative Medicine Frontier Research (NSC101-2321-B-039-001, Taiwan).

References

1. Kim VN. MicroRNA biogenesis: coordinated cropping and dicing. *Nature Rev Mol Cell Biol.* 2005; 6:376–385. [PubMed: 15852042]
2. van Kouwenhove M, Kedde M, Agami R. MicroRNA regulation by RNA-binding proteins and its implications for cancer. *Nature Rev Cancer.* 2011; 11:644–656. [PubMed: 21822212]
3. Lu J, et al. MicroRNA expression profiles classify human cancers. *Nature.* 2005; 435:834–838. [PubMed: 15944708]
4. Leung AK, Sharp PA. MicroRNA functions in stress responses. *Mol Cell.* 2010; 40:205–215. [PubMed: 20965416]
5. Pouyssegur J, Dayan F, Mazure NM. Hypoxia signalling in cancer and approaches to enforce tumour regression. *Nature.* 2006; 441:437–443. [PubMed: 16724055]
6. Gould GW, Lippincott-Schwartz J. New roles for endosomes: from vesicular carriers to multi-purpose platforms. *Nature Rev Mol Cell Biol.* 2009; 10:287–292. [PubMed: 19277045]
7. Mosesson Y, Mills GB, Yarden Y. Derailed endocytosis: an emerging feature of cancer. *Nature Rev Cancer.* 2008; 8:835–850. [PubMed: 18948996]
8. Cikaluk DE, et al. GERp95, a membrane-associated protein that belongs to a family of proteins involved in stem cell differentiation. *Mol Biol Cell.* 1999; 10:3357–3372. [PubMed: 10512872]
9. Eulalio A, Huntzinger E, Izaurralde E. Getting to the root of miRNA-mediated gene silencing. *Cell.* 2008; 132:9–14. [PubMed: 18191211]
10. Diederichs S, Haber DA. Dual role for argonautes in microRNA processing and posttranscriptional regulation of microRNA expression. *Cell.* 2007; 131:1097–1108. [PubMed: 18083100]
11. Chendrimada TP, et al. TRBP recruits the Dicer complex to Ago2 for microRNA processing and gene silencing. *Nature.* 2005; 436:740–744. [PubMed: 15973356]
12. Lemmon MA, Schlessinger J. Cell signaling by receptor tyrosine kinases. *Cell.* 2010; 141:1117–1134. [PubMed: 20602996]
13. Wang Y, et al. Regulation of endocytosis via the oxygen-sensing pathway. *Nature Med.* 2009; 15:319–324. [PubMed: 19252501]

14. Franovic A, et al. Translational up-regulation of the EGFR by tumor hypoxia provides a nonmutational explanation for its overexpression in human cancer. *Proc Natl Acad Sci USA*. 2007; 104:13092–13097. [PubMed: 17670948]
15. Reynolds AR, Tischer C, Verveer PJ, Rocks O, Bastiaens PI. EGFR activation coupled to inhibition of tyrosine phosphatases causes lateral signal propagation. *Nature Cell Biol*. 2003; 5:447–453. [PubMed: 12717446]
16. Lee OH, et al. Genome-wide YFP fluorescence complementation screen identifies new regulators for telomere signaling in human cells. *Mol Cell Proteom*. 2010; 10:M110.001628.
17. Jiang X, Huang F, Marusyk A, Sorkin A. Grb2 regulates internalization of EGF receptors through clathrin-coated pits. *Mol Biol Cell*. 2003; 14:858–870. [PubMed: 12631709]
18. Bertout JA, Patel SA, Simon MC. The impact of O₂ availability on human cancer. *Nature Rev Cancer*. 2008; 8:967–975. [PubMed: 18987634]
19. Ventura A, Jacks T. MicroRNAs and cancer: short RNAs go a long way. *Cell*. 2009; 136:586–591. [PubMed: 19239879]
20. Nicoloso MS, Spizzo R, Shimizu M, Rossi S, Calin GA. MicroRNAs – the micro steering wheel of tumour metastases. *Nature Rev Cancer*. 2009; 9:293–302. [PubMed: 19262572]
21. Leung AK, Sharp PA. MicroRNAs: a safeguard against turmoil? *Cell*. 2007; 130:581–585. [PubMed: 17719533]
22. Schirle NT, MacRae IJ. The crystal structure of human Argonaute2. *Science*. 2012; 336:1037–1040. [PubMed: 22539551]
23. Elkayam E, et al. The structure of human Argonaute-2 in complex with miR-20a. *Cell*. 2012; 150:100–110. [PubMed: 22682761]
24. Tahbaz N, et al. Characterization of the interactions between mammalian PAZ PIWI domain proteins and Dicer. *EMBO Rep*. 2004; 5:189–194. [PubMed: 14749716]
25. Maniataki E, Mourelatos Z. A human, ATP-independent, RISC assembly machine fueled by pre-miRNA. *Genes Dev*. 2005; 19:2979–2990. [PubMed: 16357216]
26. Tsutsumi A, Kawamata T, Izumi N, Seitz H, Tomari Y. Recognition of the pre-miRNA structure by *Drosophila* Dicer-1. *Nature Struct Mol Biol*. 2011; 18:1153–1158. [PubMed: 21926993]
27. Suzuki HI, et al. Modulation of microRNA processing by p53. *Nature*. 2009; 460:529–533. [PubMed: 19626115]

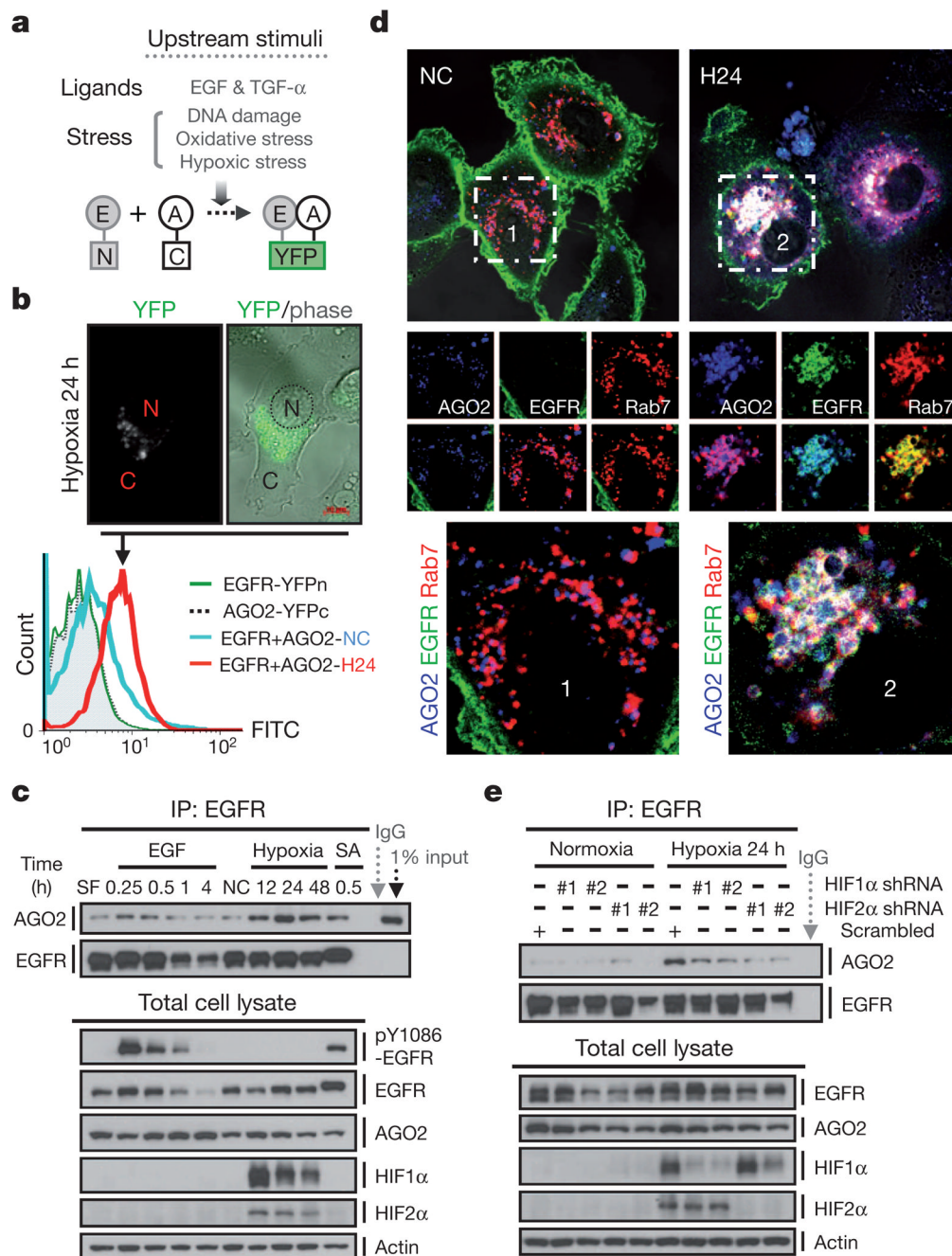


Figure 1. EGFR interacts with AGO2 in response to hypoxia

a, Split-half-YFP-fused EGFR and AGO2 were stably expressed in HTC-1080 cells to screen for upstream stimuli that might trigger EGFR–AGO2 interaction. E, EGFR; A, AGO2. **b**, Top, representative live-cell image. N, nuclear; C, cytoplasmic. Bottom, fluorescence-activated cell sorting (FACS) analysis of HTC-1080 stable transfectants as indicated. FITC, fluoresce in isothiocyanate. **c**, Immunoprecipitation and western blot analysis of HeLa cells in response to different stimuli. EGF, 20 ng ml⁻¹; SA (sodium arsenite), 500 μ M; hypoxia, 1% O₂. **d**, Confocal microscopy analysis of live HeLa cells as indicated. Rab7, a marker for late endosomes. Regions 1 and 2 at top are shown in

magnified view at bottom. NC, normoxia; H24, hypoxia 24 h. e, Immunoprecipitation and western blot analysis of HeLa stable transfectants expressing HIF1/2 α shRNAs.

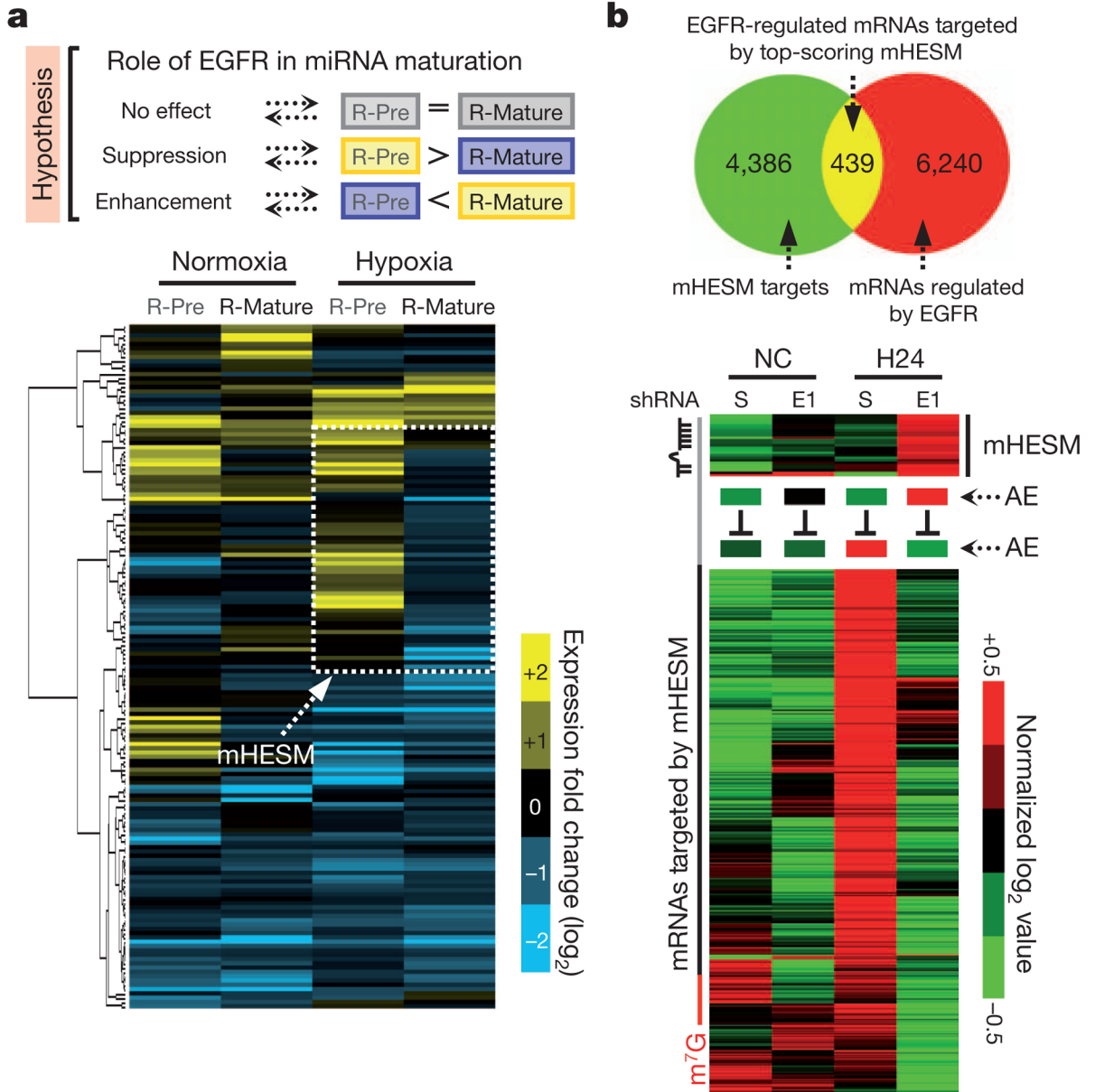


Figure 2. EGFR modulates miRNA maturation in response to hypoxia

a, Top, proposed role of EGFR in miRNA maturation. Bottom, hierarchical clustering analysis of R-Pre (\log_2 [precursor miR (scrambled)] – \log_2 [precursor miR (EGFR shRNA-E1)]) and R-Mature (\log_2 [mature miR (scrambled)] – \log_2 [mature miR (EGFR shRNA-E1)]) identified one distinct cluster of miRNAs whose maturation was suppressed by EGFR under hypoxia. We define this subcluster as mHESM. **b**, Top, Venn diagram highlighting the mRNAs that are regulated by EGFR and likely to be targeted by top-scoring mHESM (those for which R-Pre – R-Mature ≥ 0.8 and R-Mature ≤ -0.4). Bottom, EGFR-mediated suppression of top-scoring mHESM concurrent with the upregulation of targeting mRNAs in response to hypoxia. AE, average expression.

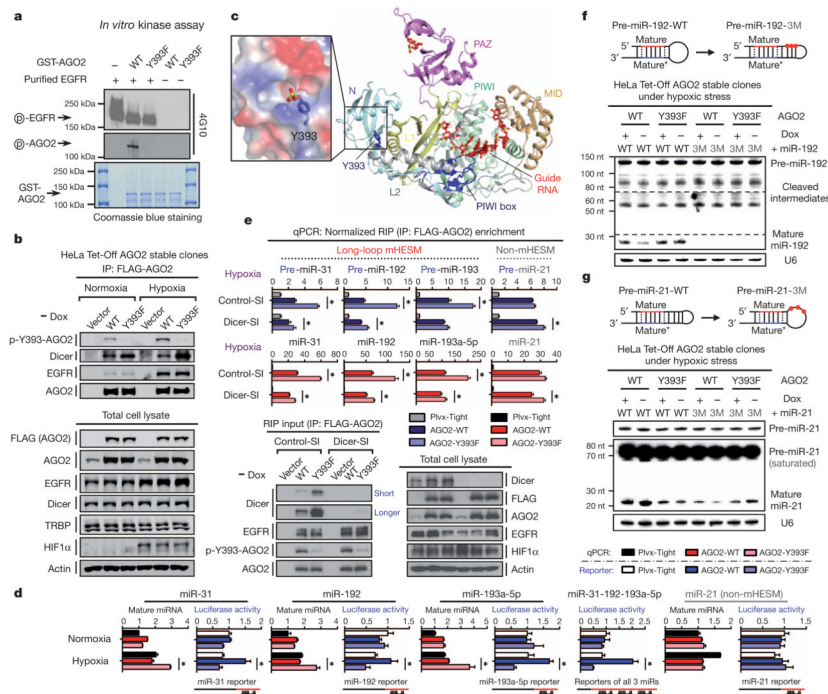


Figure 3. EGFR phosphorylates AGO2 at Tyr 393 to suppress the maturation of long-loop mHESM in response to hypoxia

a, *In vitro* kinase assay detected by 4G10 antibody. **b**, Immunoprecipitation and western blot analysis of HeLa Tet-Off-inducible AGO2 stable clones. **c**, Relative position of Tyr 393 in the structure of human AGO2 with bound guide RNA^{22,23}. The N (cyan), linker L1 (yellow), PAZ (violet), linker L2 (grey), MID (orange) and PIWI (green) domains are shown in ribbon representation, and the co-purifying guide RNA (red) is depicted in stick representation. Tyr 393 and the PIWI box are highlighted in blue. The expanded boxed segment highlights the electrostatic surface around Tyr 393, including a modelled phosphate attached to Tyr 393. **d**, Normalized expression of miRNA and corresponding luciferase activity of miR reporters ($n = 4$). **e**, RNA-binding protein immunoprecipitation (RIP) enrichment of precursor and mature miRNAs ($n = 3$). qPCR, quantitative PCR. **f, g**, Northern blot analysis as indicated. Dashed lines indicate different exposure times. RNA integrity was examined by ethidium bromide staining (Supplementary Figs 32 and 33). Data represent mean \pm s.d.; * $P < 0.05$, t -test.

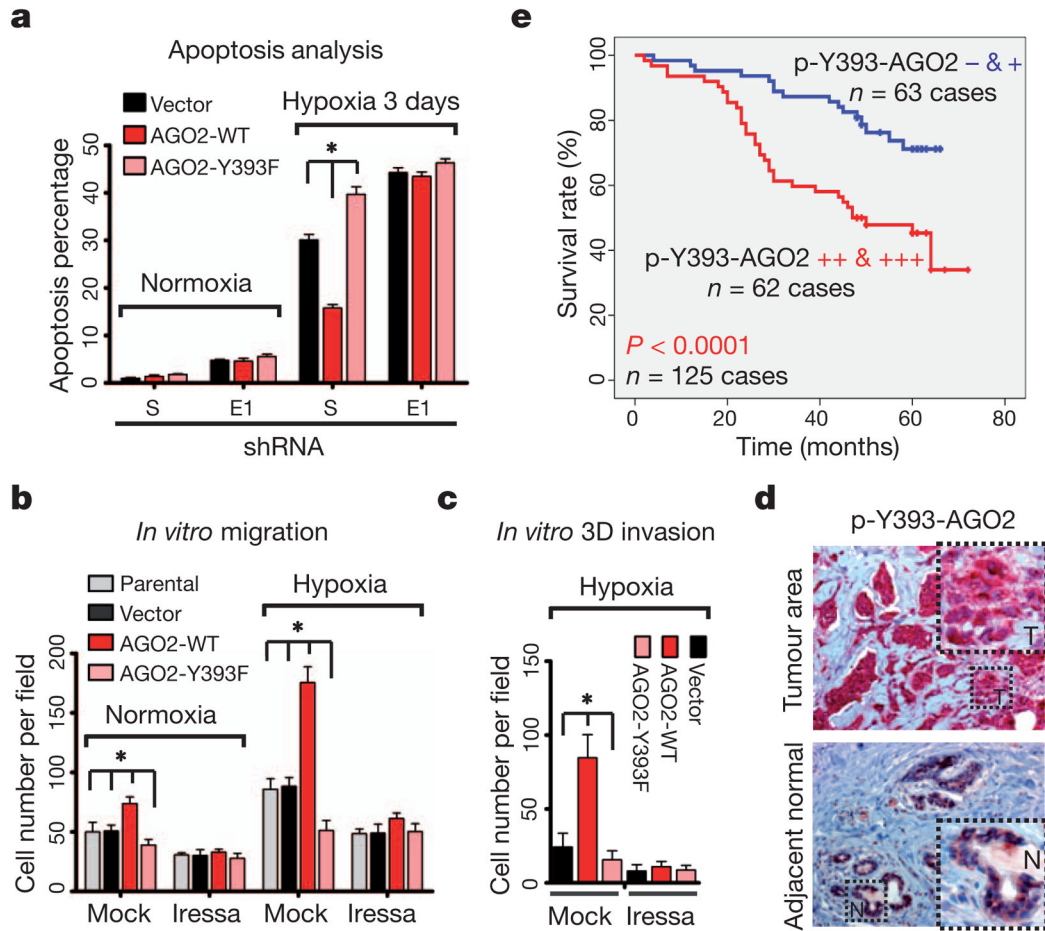


Figure 4. p-Y393-AGO2 enhances cell survival and invasiveness under hypoxia and correlates with poorer overall survival in breast cancer patients

a. Cell apoptosis analysed by FACS ($n = 3$). **b.** *In vitro* migration assay. Result was calculated on the basis of five randomly selected fields per membrane in triplicate ($n = 3$). **c.** *In vitro* three-dimensional invasion assay ($n = 5$). **d.** Representative images of immunohistochemical staining of p-Y393-AGO2 in human breast tumour and its adjacent normal tissue. **e.** Correlation between p-Y393-AGO2 and overall survival in breast cancer patients ($n = 125$). $P < 0.0001$, Kaplan–Meier survival analysis. All data represent mean \pm s.d.; * $P < 0.05$, t -test.